

# Table of Contents

CHAPTER 1 .....	1
INTRODUCTION .....	1
1.1 Background of Study.....	1
1.2 Problem Statement .....	2
1.3 Objective .....	2
1.4 Scope of Study .....	3
1.5 Feasibility of Project .....	3
CHAPTER 2 .....	4
LITERATURE REVIEW AND THEORY .....	4
2.1 Corrosion.....	4
2.2 Stainless steel .....	5
2.3 Effects of sintering atmospheres on the corrosion behavior .....	7
CHAPTER 3 .....	9
METHODOLOGY .....	9
3.1 Research methodology .....	9
3.2 Project activities .....	9
3.3 Project gantt chart and key milestone .....	10
3.4 Experimental methodology .....	11
3.4.1 Samples preparation.....	11
3.4.2 Surface roughness .....	12
3.4.3 Samples cutting.....	12
3.4.4 Weighing.....	13
3.4.5 pH measuring.....	13
3.4.6 Field emission scanning electron microscope (FESEM).....	14
3.5 Procedure.....	15
3.5.1 Weight loss method.....	16

CHAPTER 4 .....	17
RESULTS AND DISCUSSION .....	17
4.1    Weight loss test .....	17
4.2    Material characterization.....	19
4.2.1    FESEM analysis on hydrogen sintering.....	19
3.2.2    FESEM analysis on nitrogen sintering .....	21
3.2.3    FESEM analysis on vacuum sintering .....	23
4.3    The effect of sintering atmosphere on the corrosion behavior.....	25
4.4    Surface roughness analysis.....	26
CHAPTER 5 .....	27
CONCLUSION AND RECOMMENDATION.....	27
REFERENCES .....	28
APPENDICES .....	30

# CHAPTER 1

## INTRODUCTION

### 1.1 Background of Study

316L stainless steel is frequently used because of its combination of strength with corrosion resistance. 316L SS is an extra-low carbon austenitic steel containing chromium nickel and molybdenum [1]. This addition increases general corrosion resistance, improves resistance to pitting from chloride environment, and provides increased strength at elevated temperature, and therefore has wide applications in industry.

316L stainless steel parts can also be produced by traditional powder metallurgy (PM). Nevertheless, PM parts are limited in terms of the shape complexity and production efficiency, not to mention the poor mechanical properties and corrosion resistance caused by large porosity and density gradients [2].

Powder injection molding (PIM) is the most commonly used manufacturing process for the fabrication of metallic and ceramics part. A wide variety of products are manufactured using injection molding. The PIM is divided into four production steps. First is the feedstock preparation. Second is the injection molding takes place. Third is the debinding and the fourth step is sintering process. Finally the sample or parts is formed. Process flow is shown in Figure 1-1.

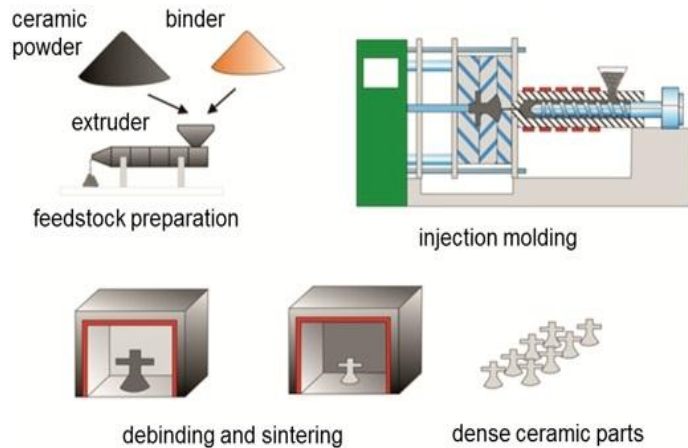


**Figure 1-1: Powder Injection Molding Process [10]**

## 1.2 Problem Statement

Stainless steels are used in many applications such as transportation, medical, oil and gas, architectural and pharmaceutical due to excellent combination of mechanical properties and corrosion resistance.

Stainless steels 316L is commonly recommended for medical applications due to its low cost, excellent combination of mechanical properties and corrosion resistance as compared to other alloys. In the human body, the presence of chloride ions generates localized corrosion. Eventually, corrosion does not withstand with chloride environment. Therefore, additional coatings and heat treatment are the best answer to improve the corrosion resistance [3].

## 1.3 Objective

The primary aim of this project is to study the general corrosion behavior of various sintered atmosphere of 316L stainless steel. The aim could be achieved through the following objective:

- To study the effects of sintering atmosphere and solid loading on corrosion behavior of powder injection molded 316L SS in Ringer's solution.

#### **1.4 Scope of Study**

In order to analyze the corrosion behavior of 316L stainless steel in three different sintering atmospheres, this study will involve: weight loss tests, Atomic and Field-Emission Scanning Electron Microscope (FESEM).

#### **1.5 Feasibility of Project**

The feasibility for this project to be completed within the time limit is 14 weeks. This report must be accomplished in time. This project required experimental work to study the corrosion behavior. All of the objectives can be achieved if the procedures follow closely.

## **CHAPTER 2**

### **LITERATURE REVIEW AND THEORY**

#### **2.1 Corrosion**

Corrosion can be defined as decaying or destruction of a material caused by the environment in which the material resides [4]. For example, steel rusts when immersed in seawater. Corrosion has been classified in many different forms. Each form of attack has a specific arrangement of anodes and cathodes and the corrosion which occurs has a specific location and pattern [5]. Some of the common forms of corrosion are listed below:

- i. Uniform / General corrosion
- ii. Galvanic corrosion
- iii. Crevice corrosion
- iv. Pitting
- v. Stress-corrosion cracking
- vi. Erosion corrosion

In the previous literatures, there were investigations on the corrosion behavior of cast 316L stainless steel [6]. Corrosion prevention of PIM 316L stainless steel is significantly important for biomedical application. The presence of chloride ion in the human body can generate localized corrosion. There are consequences to human body due to this problem such as allergic and hypersensitivity reaction. The solutions of these problems are by minimizing the surface treatments, reinforcement of noble metals or carbides and oxide dispersion with yttria [7].

## **2.2 Stainless steel**

When the first stainless steels were developed in the early 1900s, Harry Brearly of Sheffield found that steel that had been alloyed with a sufficiently high level of chromium was not susceptible to attack from etching acids or moisture [8]. The first stainless steel was martensitic with 0.24% carbon and 12.8% chromium. Stainless steels achieved their stainless characteristics through the formation of an invisible and adherent chromium rich oxide film. Type 316L is the low carbon version of 316 stainless steels [8].

316L stainless steels are usually manufactured by powder injection molding process. The 316L composition is frequently used because of its combined strength and corrosion resistance. In which type 316L is an extra-low carbon austenitic chromium nickel stainless steel containing molybdenum [8]. This addition increases general corrosion resistance, improves resistance to pitting from chloride ion solutions, and provides increased strength, and therefore has wide applications in industry.

Compared to chromium-nickel austenitic stainless steels, 316L stainless steel higher creep, stress to rupture and tensile strength at elevated temperature. The chemical composition, mechanical properties and physical properties of 316L stainless steels are shown below:

**Table 2-1: Chemical Composition of 316L Stainless Steels [9]**

<b>Element</b>	<b>Weight percentage (%)</b>
Carbon	0.0030
Manganese	2.00
Silicon	0.75
Chromium	16.00 18.00
Nickel	10.00 14.00
Molybdenum	2.00 3.00
Phosphorus	0.045
Sulfur	0.030
Nitrogen	0.10
Iron	Bal.

**Table 2-2: Mechanical Properties of 316L Stainless Steels [9]**

<b>Mechanical Properties</b>	<b>Type 316L</b>
Tensile Strength	485 (MPa) min
Yield Strength 0.2% Proof	170 (MPa) min
Elongation	40 (% in 50mm) min
Hardness Rockwell B	95 (HR B) max
Hardness Brinell	217 (HB) max

**Table 2-3: Physical Properties of 316L Stainless Steels [9]**

<b>Physical Properties</b>	<b>Type 316L</b>
Melting range	1375-1400 <sup>o</sup> C
Density	0.29 lb/in <sup>3</sup> (8.027 g/cm <sup>3</sup> )
Modulus of Elasticity in Tension	29 x 10 <sup>6</sup> psi (200 GPa)
Modulus of Shear	11.9 x 10 <sup>6</sup> (82 GPa)

### 2.3 Effects of sintering atmospheres on the corrosion behavior

From the previous researchers, several investigations on the corrosion behavior of cast 316L stainless steel had been carried out. Hao He *et al* said that the corrosion rates increases first, and then decreases with increasing time [10]. From the graph shown in Figure 2-1, the trend of all the curves indicate similar trends that the corrosion rates increases with increasing time in the initial 25 hour, and then it decreases from 25 hour to 88 hour for sintering under various temperatures and atmospheres.

Based on what Hao He said about the results, it was observed that vacuum sintered test samples showed minimum corrosion attack [10]. In case of test samples sintered in inert atmosphere showed higher corrosion rate.

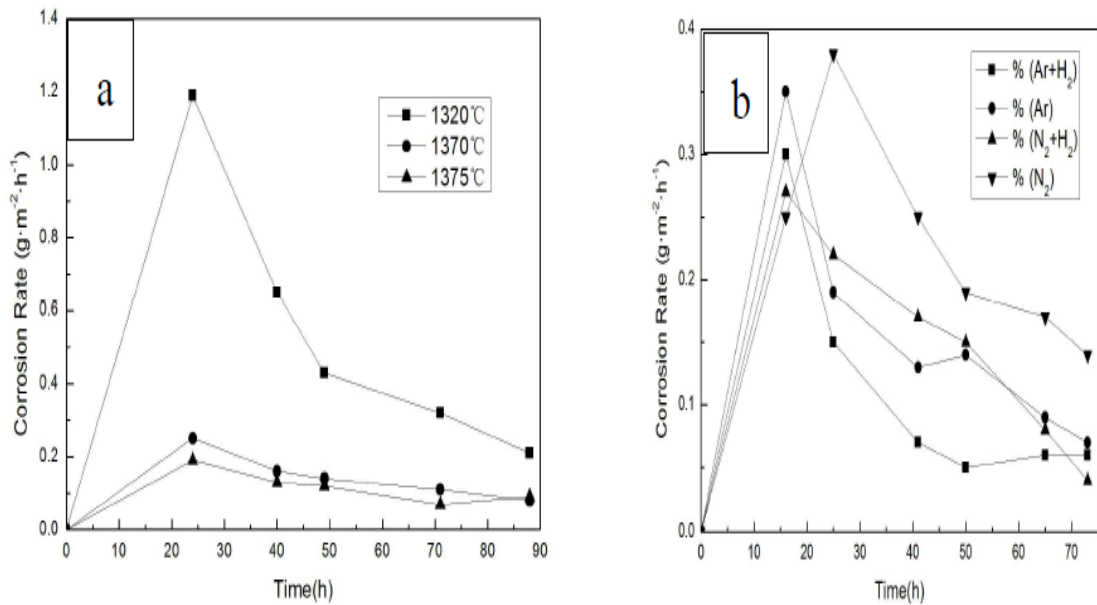


Figure 2-1: Corrosion rate of 316L SS sintered (a) at various temperatures and (b) under various atmospheres [10]

Hao He *et al* studied the corrosion behavior between specimens sintered in different atmospheres is consistent with the corrosion morphology [10]. Due to a weak localized corrosive attack, grain boundaries of specimens sintered under Ar + H<sub>2</sub> are not fully corroded. Whereas some corrosion trace in the shape of notching curve as well as separated grain boundaries can be clearly seen in N<sub>2</sub> sintered specimens, reflecting a strong localized corrosive attack. A high porosity with large, irregular and interconnected pores can be clearly seen when sintering under N<sub>2</sub> atmosphere.

Therefore, the importance of sintering is discussed on its effect on corrosion resistance. Previous studies have shown that the important factors of the sintering cycle are heating rate, sintering time, sintering temperature and sintering atmosphere [11]. These factors can affect the microstructure, pore size and shape, final density and final nitrogen content of the sintered stainless steel. An understanding of the effects of the sintering factors on the final density and mechanical properties can be used to optimize the sintering process.

## CHAPTER 3 METHODOLOGY

### 3.1 Research methodology

Before executing the project, a thorough research had been conducted to exposure self to the knowledge of corrosion behavior of 316L stainless steel. After that, experiments will be conducted to test the corroded samples. The experiment will mostly involve in the laboratory in Block 16, Block 17 and Block P.

### 3.2 Project activities

The project activities are summarized in Figure 3 below.

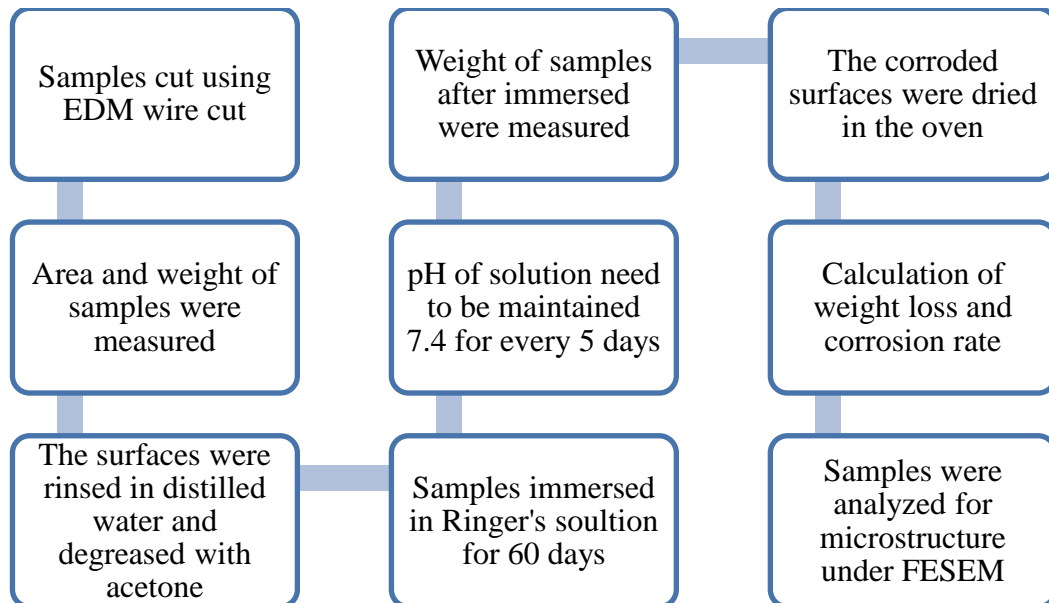


Figure 3-1: Flow chart of project activities

### 3.3 Project gantt chart and key milestone

ACTIVITY	FYP 1				FYP 2			
	MAY	JUNE	JULY	AUG	SEPT	OCT	NOV	DEC
Study the literature review								
Research methodology								
Extended proposal			●	●				
Experimental work – corrosion test							●	
Analyze result								●

Milestone		
A	Extended proposal	●
B	Final report FYP 1	●
C	Poster presentation	●
D	Viva presentation & Report submission	●

### 3.4 Experimental methodology

#### 3.4.1 Samples preparation

The experimental works will be carried out in two parts for this project. The first part is to prepare the samples needed for experiment. There are four solid loading formulations involve in this experiment which are 60vol%, 65vol%, 67vol% and 69vol%. These four formulations were sintered in 3 different atmospheres; hydrogen, nitrogen and vacuum. The detailed formulation is as described in the following table.

Table 3-1: Samples formulation

No of samples	Solid loading of samples
HYDROGEN	
1	67F
2	67F
3	69F
4	69F
5	60F
6	60F
7	65F
8	65F
NITROGEN	
1	67F
2	67F
3	69F
4	69F
5	60F
6	60F
7	65F
8	65F
VACUUM	
1	67F
2	69F
3	60F
4	65F

### 3.4.2 Surface roughness

The samples were tested for its surface roughness before the cutting process. There are important parameters need to be considered which is “Ra”. Ra is commonly defined as the arithmetic average roughness.

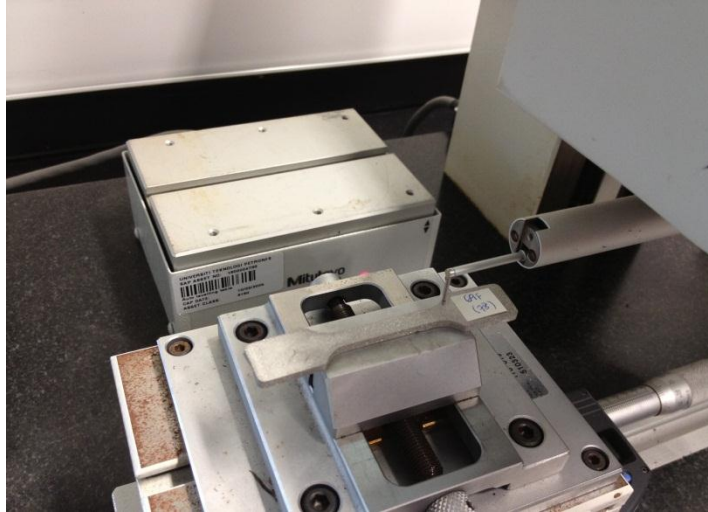


Figure 3-2: Surface of the samples been measured

### 3.4.3 Samples cutting

Samples were cut into 5 small pieces using electric discharge machine (EDM) wire cut. The wire-cut process uses water as its dielectric fluid. The water also flushes the cut debris away from the cutting zone.



Figure 3-3: EDM wire cut for samples cutting

### 3.4.4 Weighing

The samples were weighed before and after immersed in the Ringer's solution. The purpose of this activity is to get the weight loss results at the end of the experiment.

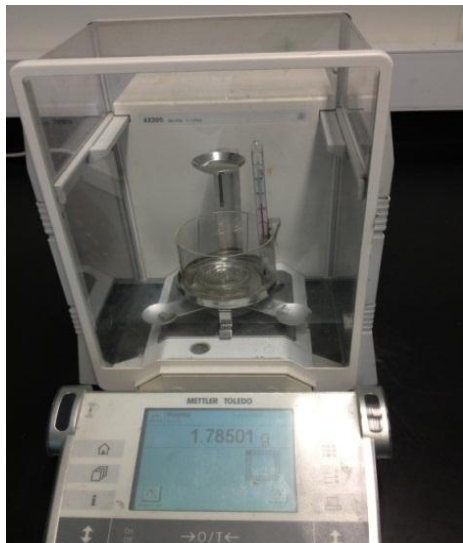


Figure 3-4: Analytical lab balance scale for samples weighing

### 3.4.5 pH measuring

The samples were immersed in the Ringer solution for 60 days and throughout the period, pH of the solution need to be maintained at 7.4.



Figure 3-5: Maintaining the pH 7.4 of solution

### 3.4.6 Field emission scanning electron microscope (FESEM)

After finished with the immersion activity in the Ringer solution, the samples were then examined for FESEM analysis. The samples needed to be dried in the oven for 3 hours before it were taken to the FESEM machine.



**Figure 3-6: FESEM used to analyze the microstructure of samples**

### 3.5 Procedure

The second part of this experiment is to prepare the solutions needed. There are three solutions which are:

- 1M HNO<sub>3</sub>
- 1M NaOH
- Ringer's solution

- **Preparation of 1M HNO<sub>3</sub>**

To prepare 1 Liter of 1 M HNO<sub>3</sub>, measure 63 ml of 16 M concentrated acid in a fume cupboard and add it to 937 ml of distilled water. Magnetic stirrer is used to mix the acid.

- **Preparation of 1M NaOH**

To prepare 1 Liter of 1 M NaOH, dissolve 40 gram (1 mole) of NaOH (sodium hydroxide) in 1 L of distilled water. It is more convenient to prepare an approximate NaOH solution at approximately 1 M strength, as 40 g of NaOH is a convenient quantity to weight.

Note: Only an approximate concentration of NaOH solution can be prepared, which will then have to be standardized.

- **Preparation of Ringer's solution**

To prepare 1 Liter of Ringer's solution, dissolve 8.00 g/l NaCl, 0.2 g/l NaHCO<sub>3</sub>, 0.24 g/l CaCl<sub>2</sub>, 6H<sub>2</sub>O, 0.42 g/l KCl. The solution was prepared with analytically pure reagents and doubly distilled water. Magnetic stirrer is used to mix the solution.

### 3.5.1 Weight loss method

The samples for weight loss tests were prepared in accordance to the procedure recommended by ASTM G31-72. The samples were cut into 5 pieces. They were rinsed in acetone and distilled water to remove dirt, oils and possible product formed on the surface of the samples.

The samples were fully immersed in Ringer's solution at  $37 \pm 1^\circ\text{C}$  after the initial weight had been recorded. This temperature was selected for considering the human body temperature. The pH of the solution was maintained 7.4 by using 1M solution of  $\text{HNO}_3$  and  $\text{NaOH}$ . The weight of samples were taken right after 60 days to measure the changes in weight, which was obtained after cleaning the surfaces of the samples. The mathematical formula was used to study the corrosion rates of the samples after the weight loss measurements, namely:

$$\Delta W = \frac{W_2 - W_1}{W_1} \times 100\%$$

Where  $\Delta W$  = Weight loss

$W_1$  = sample weight before water immersing

$W_2$  = sample weight after water immersing

$$R = \frac{\Delta W}{A \times t}$$

Where  $R$  = corrosion rate

$\Delta W$  = weight loss (g)

$A$  = sample area ( $\text{m}^2$ )

$t$  = time (h)

## **CHAPTER 4**

### **RESULTS AND DISCUSSION**

This chapter covers the results obtained from the phase identification studies, microstructural and morphological studies of 316L stainless steels and their corrosion behavior with detailed discussion.

#### **4.1 Weight loss test**

The corrosion behavior of the metal was first studied using weight loss measurements in Ringer's solution. The corrosion behavior of the metal in Ringer's solution was studied for 60 days. Generally, hydrogen sintered test samples showed the highest corrosion rate compared to vacuum sintered as shown in Figure 4-1 which may be considered due to the excessive amounts of carbon and nitrogen can give rise to the formation of chromium carbides and chromium nitride, with negative effects on corrosion resistance [7]. It was observed that vacuum sintered samples showed the minimum corrosion rate. Whereas nitrogen sintered samples corrosion rate showed higher than vacuum sintered samples but less than hydrogen sintered samples due to the reduction of porosity and termination of nitrogen gas which helps to improve the corrosion resistance [7].

Table 4-1: Corrosion rate of various sintered atmosphere in different solid loading

Formulation (vol%)	Corrosion rate (mpy)		
	Vacuum	H <sub>2</sub>	N <sub>2</sub>
60	0.074	0.712	0.084
65	0.083	0.671	0.059
67	0.049	0.870	0.055
69	0.028	0.694	0.099

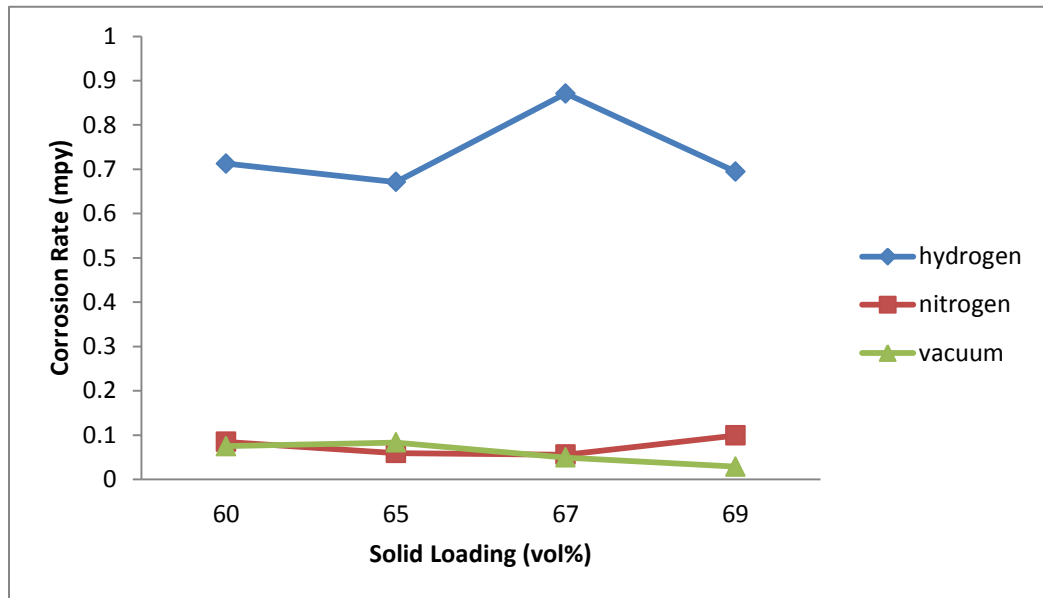


Figure 4-1: Corrosion of PIM 316L SS in Ringer solution after 60 days for samples sintered in various atmospheres

## 4.2 Material characterization

### 4.2.1 FESEM analysis on hydrogen sintering

The hydrogen sintered has been observed under Field Emission Scanning Electron Microscope and the micrograph is shown in Figure 4-2.

Immersion tests were carried out to investigate the corrosion behavior of 316L stainless steels in Ringer's solution. Figure 4-2 shows the FESEM micrograph of hydrogen sintered after 60 days of exposure in Ringer's solution. Figure 4-2 revealed that the microstructure of 316L stainless steels showed carbides and corrosion attach. The carbides were found to be standing in relief and showed slightly rounding at the exposed periphery of the carbides but did not show signs of any significant fracturing or cracking.

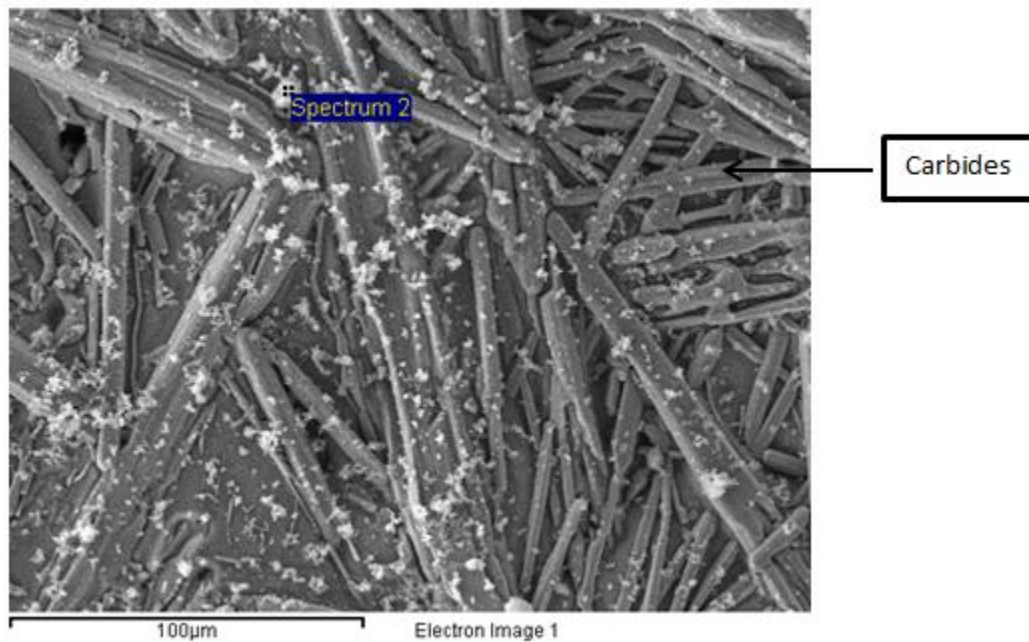


Figure 4-2: FESEM micrograph of hydrogen sintered 316L stainless steel showing corrosion attach and carbides

The EDX observed is shown in Figure 4-3. EDX was taken to identify the components of corrosion products film formation on the stainless steels surfaces. In the second spectrum represented the light phase, oxygen, silica, chlorine, calcium, chromium, iron and nickel. Other element observed on this spectrum was sodium. The element detected on the dark phase was molybdenum. Element detected in the third spectrum were similar to the elements observed with the second spectrum. However, in the first spectrum there were absent of elements molybdenum.

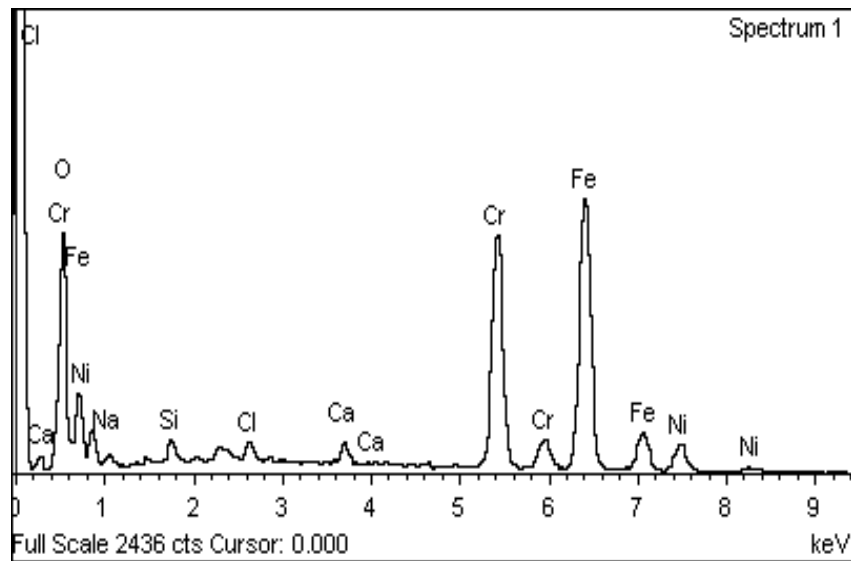


Figure 4-3: EDX analysis showing the presence of O<sub>2</sub> and Fe with metals that formed the Fe<sub>2</sub>O<sub>3</sub> (rusting activity takes place)

### 3.2.2 FESEM analysis on nitrogen sintering

The nitrogen sintered has been observed under Field Emission Scanning Electron Microscope and the micrograph is shown in Figure 4-4.

Immersion tests were carried out to investigate the corrosion behavior of 316L stainless steels in Ringer's solution. Figure 4-4 shows the FESEM micrograph of nitrogen sintered after 60 days of exposure in Ringer's solution. Figure 4-4 revealed that the microstructure of 316L stainless steels showed carbides, nitride, and corrosion attack. Porosity was observed on the surface of the samples as indicated in Figure 4-4. Some corrosion trace in the shape of notching curve as well as separated grain boundaries can be clearly seen, reflecting a strong localized corrosive attack. Under nitrogen atmosphere, a high porosity with large, irregular and interconnected pores can be clearly seen.

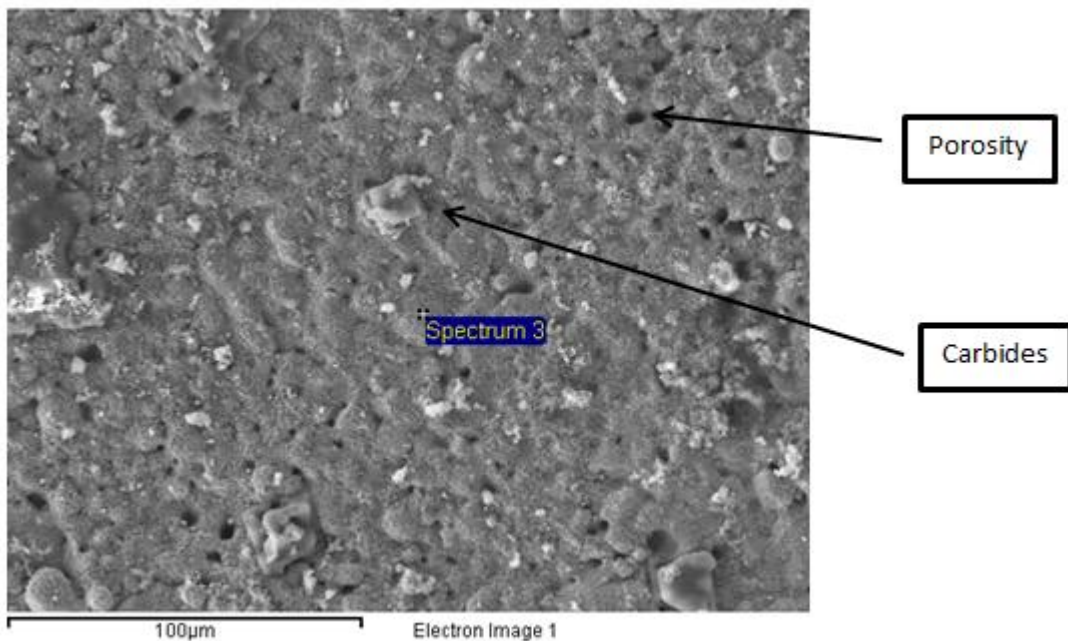


Figure 4-4: FESEM micrograph of nitrogen sintered 316L stainless steel showing the carbides, corrosion attack and porosity

The EDX observed is shown in Figure 4-5. EDX was taken to identify the components of corrosion products film formation on the stainless steels surfaces. In the first spectrum which represented the light phase, chromium, iron, nickel and molybdenum. The other elements were aluminum, silica and calcium. Whereas in the third spectrum which represented the dark phase, oxygen, sodium, chlorine, chromium and iron.

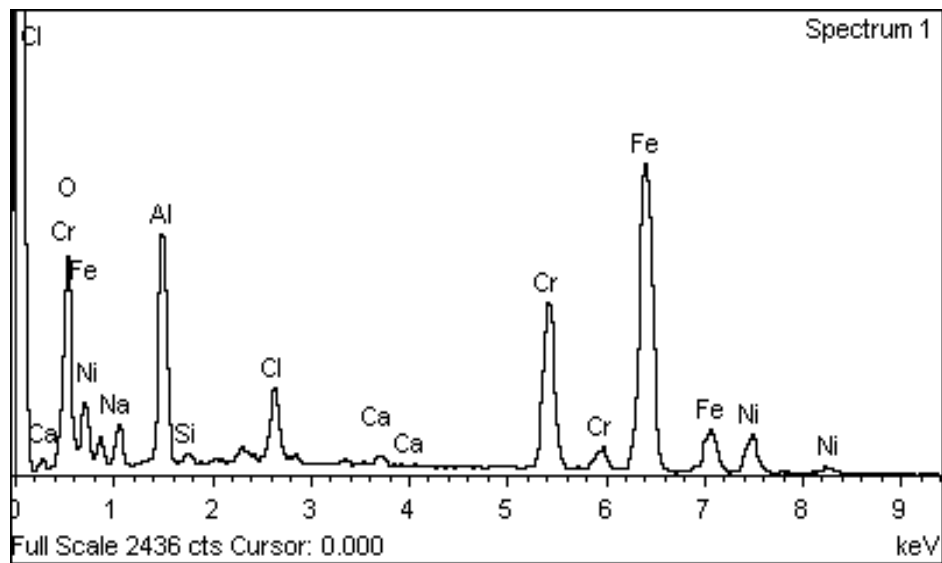
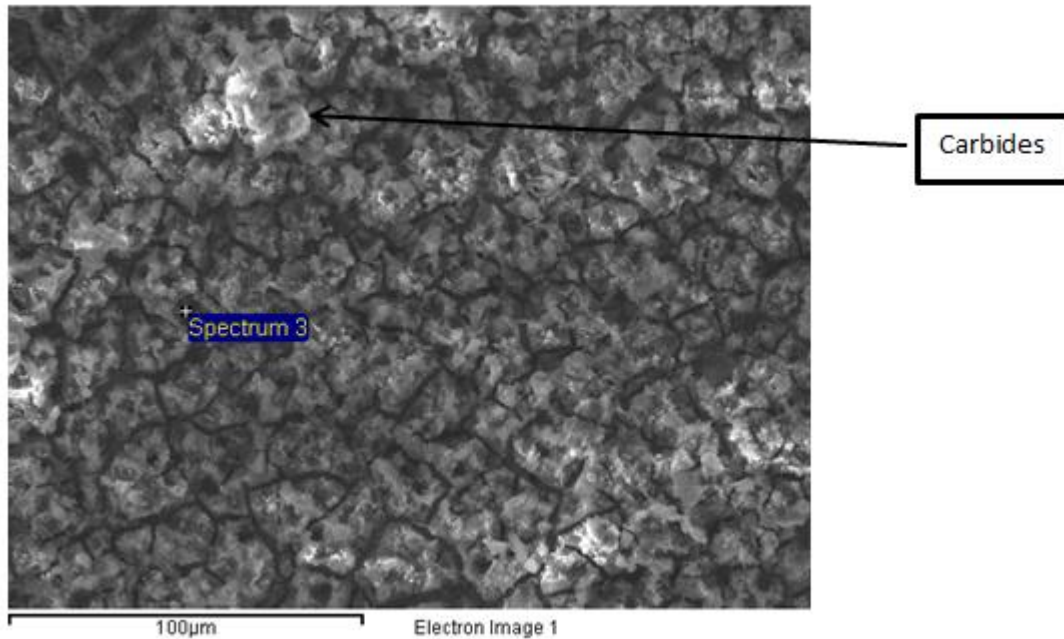


Figure 4-5: EDX analysis showing the presence of O<sub>2</sub> and Fe with metals that formed the Fe<sub>2</sub>O<sub>3</sub> (rusting activity takes place)

### 3.2.3 FESEM analysis on vacuum sintering

The vacuum sintered has been observed under Field Emission Scanning Electron Microscope and the micrograph is shown in Figure 4-6.

Immersion tests were carried out to investigate the corrosion behavior of 316L stainless steels in Ringer's solution. Figure 4-6 show the FESEM micrograph of vacuum sintered after 60 days of exposure in Ringer's solution. Figure 4-6 revealed that the microstructure of 316L stainless steels showed the corrosion attack. Less corrosion was observed in vacuum sintered parts due to the less evaporation of chromium ion that settle down on the surface of the test samples and formed the passive oxide layer at the surface of the part that protect from corrosion in chloride environment.



**Figure 4-6: FESEM micrograph of vacuum sintered 316L stainless steel showing the carbides and some corrosion attack**

The EDX observed is shown in Figure 4-7. EDX was taken to identify the components of corrosion products film formation on the stainless steels surfaces. In the second spectrum represented the light phase, oxygen, sodium, aluminum, silica, chlorine, calcium, chromium, iron and nickel. The other elements were carbon and molybdenum. Whereas in the third spectrum represented the dark phase, aluminum, chlorine, calcium, chromium, iron, nickel and molybdenum.

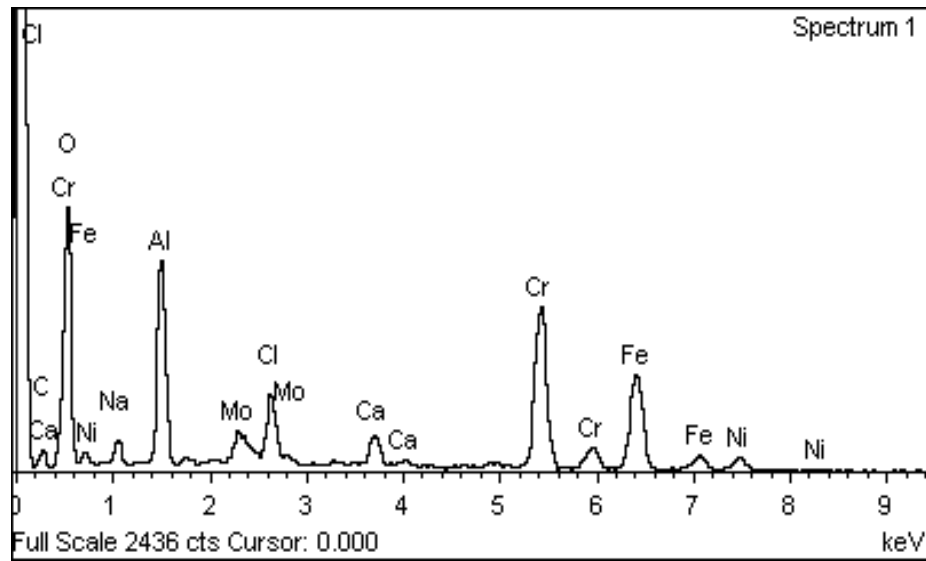


Figure 4-7: EDX analysis showing the presence of O<sub>2</sub> and C with metals that formed the oxide and carbides

### 4.3 The effect of sintering atmosphere on the corrosion behavior

The corrosion rate curves of the sintered samples at different atmospheres are shown in Figure 4-1. It can be seen that in all cases, the corrosion rates are fluctuates. The corrosion rates decreases first, then increases and decreases again. Sample sintered in vacuum has the smallest corrosion rate, reflecting a better corrosion resistance. Whereas, hydrogen sintered sample has the worst corrosion resistance because it has the largest corrosion rate. The results were also confirmed by EDX analysis that indicates the presence of nickel (Ni) in Table 4-2, which causes the corrosion.

The corrosion behavior between specimens sintered in different atmospheres is quite similar with the corrosion morphology. Grain boundaries of specimens sintered under nitrogen and vacuum are not fully corroded. Generally, the presence of aluminum is believed to be beneficial in improving the corrosion resistance of stainless steel.

In case of test samples sintered in hydrogen showed the higher corrosion rate, which also may be considered due to the presence of residual carbon during the thermal debinding process and during sintering process this carbon reacts with metals and formed carbides [13]. From the FESEM results it is concluded that the presence of carbides increased the pitting corrosion attack.

Oxygen content of the sintered samples was shown in Table 4-2. It is indicated that, the higher corrosion rate, the greater amount of oxygen in the samples. Oxygen accelerates the corrosion rate of specimens and deteriorated the corrosion resistance. It was found that lower oxygen content in pores is beneficial to enhancing the corrosion resistance.

Table 4-2: EDX analysis of test sample after corrosion sintered in different atmosphere

Atmosphere	O	Na	Al	Si	Cl	Ca	Cr	Fe	Ni	Mo	C
Hydrogen	44.27	2.23	-	2.57	2.05	1.02	3.53	32.03	12.28	-	-
Nitrogen	18.53	4.06	10.84	0.44	3.33	0.38	14.27	40.84	7.32	-	-
Vacuum	34.61	2.59	10.3	-	3.76	1.87	19.65	16.77	3.07	3.4	3.98

#### 4.4 Surface roughness analysis

Effect of surface roughness on corrosion behavior of 316L stainless steel was investigated. Experimental results showed that the surface roughness has a significant effect on the corrosion behavior and it depends on the steel type.

From data collected as shown in Table 4-3, reduction in surface roughness caused increasing in the corrosion rate values. The arithmetical mean roughness (Ra) of hydrogen sintered showed the highest value whereas for vacuum sintered the Ra value showed the least. The corrosion resistance improved as the surface roughness reduced. The fact has been proved by FESEM and EDX analysis shown in Figure 4-2 until Figure 4-7. The detailed EDX analysis is given in Table 4-2 showed the absence of carbon content in hydrogen and nitrogen compared to vacuum atmosphere.

**Table 4-3: Measurement of surface roughness**

Sintered sample	Measurement of surface roughness, Ra ( $\mu\text{m}$ )	
	Top	Bottom
Hydrogen	22.963	21.885
Nitrogen	10.891	20.718
Vacuum	13.125	5.909

## **CHAPTER 5**

### **CONCLUSION AND RECOMMENDATION**

This study concluded that:

- PIM 316L stainless steels sintered under vacuum atmosphere has the lowest porosity, nickel and aluminum content, and thus the highest corrosion resistance.
- At the same time, PIM 316L stainless steels sintered under hydrogen show the lowest corrosion resistance. This led concluded that the sintered samples in gas atmospheres are not recommended for medical applications.
- For the surface roughness analysis, results shown that reduced in surface roughness value, increases the corrosion rate.
- Formulation 65vol% showed optimum corrosion rate and this concluded that 65vol% is the finest solid loading.

Recommendation:

- It is recommended that vacuum sintering atmosphere can be successfully used in biomedical applications.
- Since the experiment only conducted for 60 days, it is suggested in next experiment the duration of the project could be extended until 90 days to observe the corrosion behavior of 316L stainless steel.

## REFERENCES

- [1] A. John Sedriks (1996) *Corrosion of Stainless Steels*, 2<sup>nd</sup> ed., A Wiley-Interscience Publication John Wiley & Sons, Inc.
- [2] Ji, C.H., Loh, N.H., Khor, K.A., Tor, S.B., 2001. Sintering study of 316L stainless steel metal injection molding parts using Taguchi method: final density. *Mater. Sci. Eng. A* 311, 74-82
- [3] Douglas C. Hansen, "Metal corrosion in the human body: the ultimate bio-corrosion scenario," *Electrochem. Soc. Interface*, 2008, vol. 17, pp. 31-34
- [4] NST Center, What is corrosion? [online], available: <http://www.nstcenter.com/writeup.aspx?title=What%20is%20Corrosion&page=TechResourcesACorrosionPrimer.html>
- [5] Corrosion doctors, Eight Forms of Corrosion [online], available: <http://corrosion-doctors.org/Corrosion-History/Eight.htm>
- [6] Hofmann, J., Michel, R., Holm, R. and Zilkens, J. (1981), Corrosion behaviour of stainless steel implants in biological media. *Surf. Interface Anal.*, 3: 110–117. doi: 10.1002/sia.740030304
- [7] Garcia, C., Martin, F., Tiedra, P.d., Garcia Cambronero, L., 2007. Pitting corrosion behavior of PM austenitic stainless steel sintered in nitrogen-hydrogen atmosphere. *Corros. Sci.* 49, 1718-1736
- [8] Jonathan Beddoes, J. Gordon Parr (1999) *Introduction to Stainless Steels*, 3<sup>rd</sup> ed., ASM International.
- [9] United Performance Metal, *316 / 316L Stainless Steel Sheet & Coil* [online], available: <http://www.upmet.com/316-chemical.shtml>

[10] Hao H., Yimin L., Dapeng L., 2011. Effect of sintering temperature and atmosphere on corrosion behavior of MIM 316L stainless steel. *Advanced Materials Research Vols. 239-242*, pp 132-136

[11] K. Erhard, S. K. Prasan (2007) *Powder Metallurgy Stainless Steels: Processing, Microstructures, and Properties*, ASM International, 1<sup>st</sup> ed., 60-100

[12] Faculty of Engineering, Science and The Built Environment, *Atoms and Molecules, an overview* [online], available:  
[http://www.lsbu.ac.uk/biology/biolchem/week\\_3.html](http://www.lsbu.ac.uk/biology/biolchem/week_3.html)

[13] Muhammad Rafi Raza, Faiz Ahmad., M.A. Omar and R.M German, “Effects of Cooling Rate on Mechanical Properties and Corrosion Resistance of Vacuum Sintered Powder Injection Molded 316L Stainless Steel,” *Journal of Materials Processing Technology*, 2012, vol. 212, pp. 164-170

# **APPENDICES**

# APPENDIX A

## SURFACE ROUGHNESS RESULT

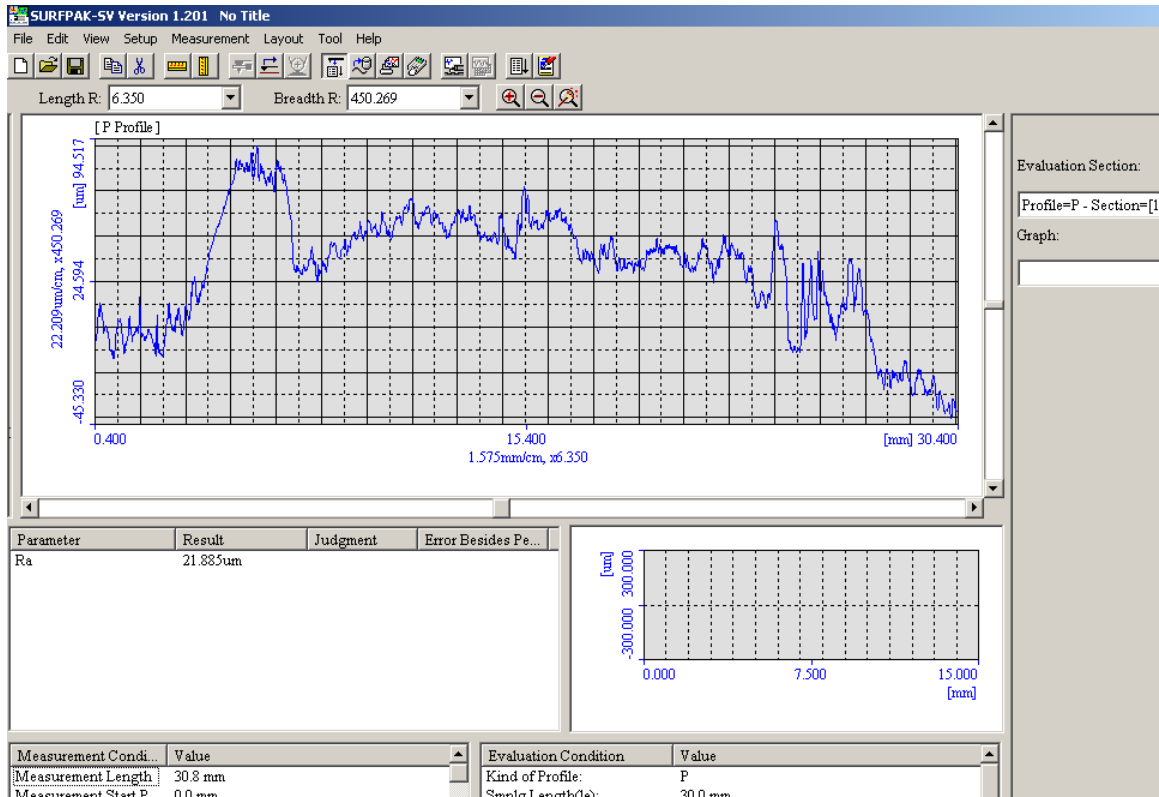


Figure A-1: Result of the surface roughness of hydrogen sintered

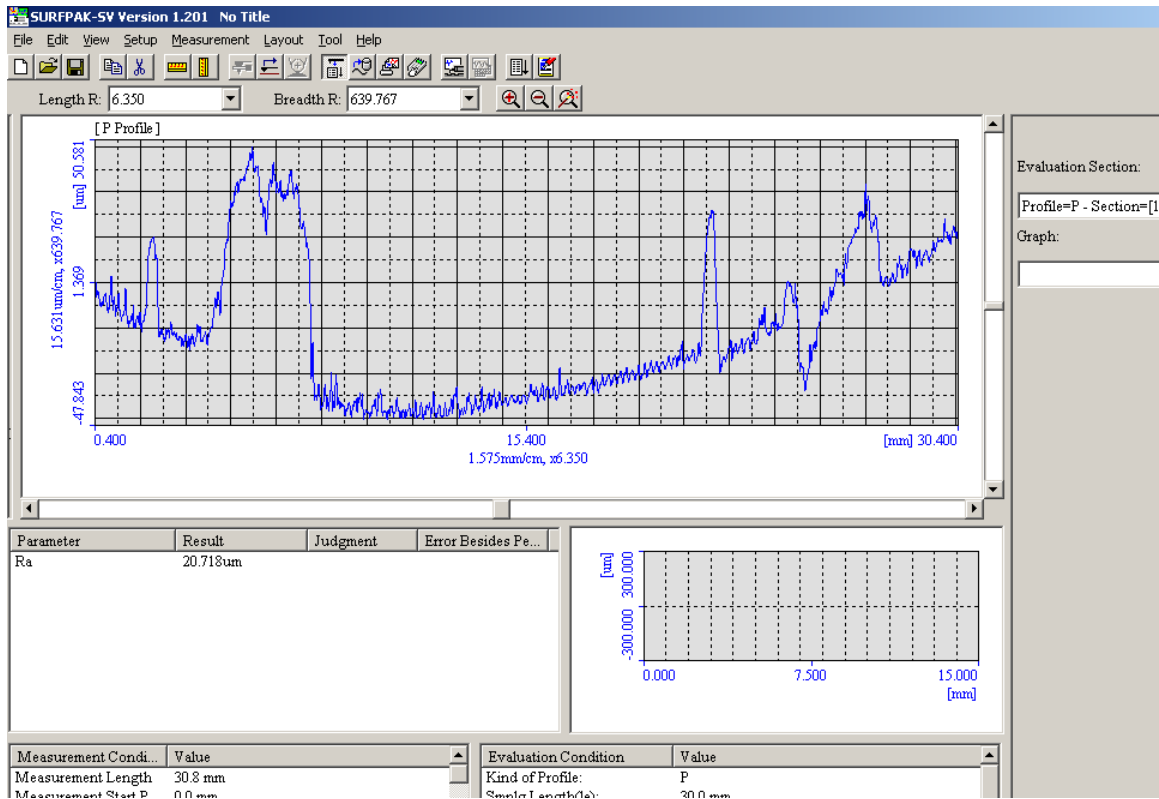


Figure A-2: Result of the surface roughness of nitrogen sintered

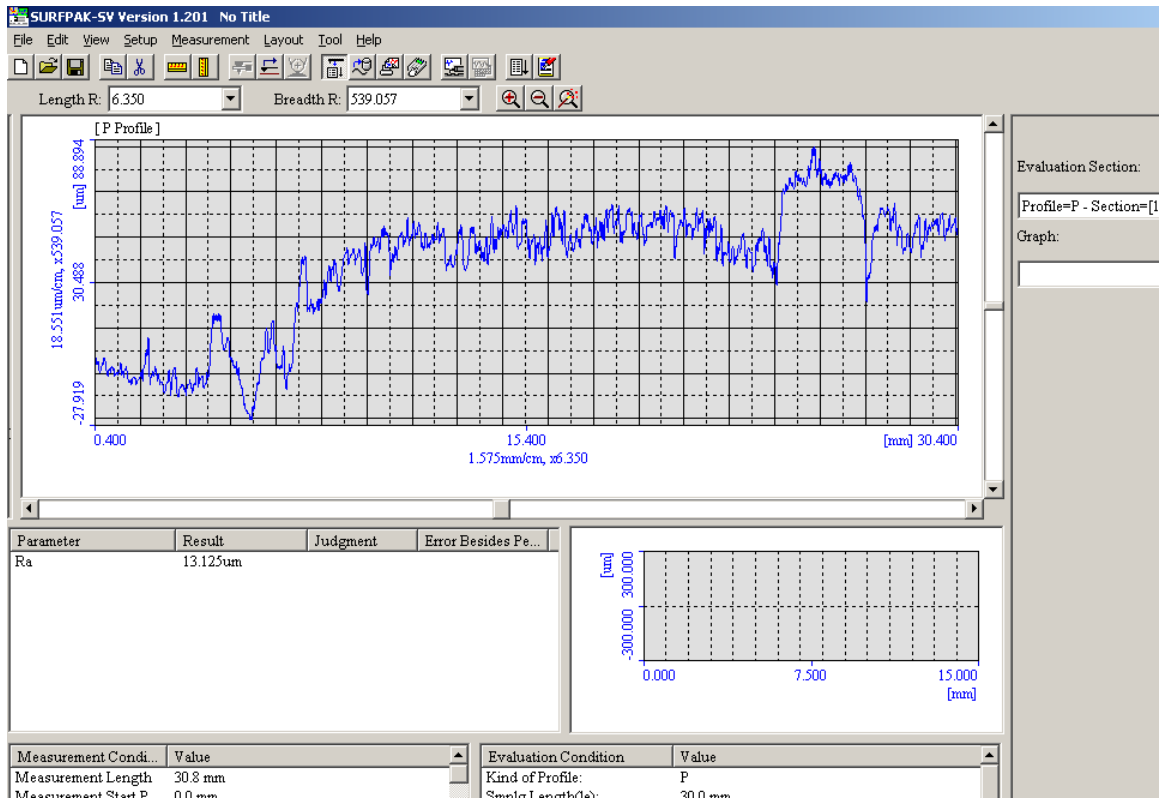


Figure A-3: Result of the surface roughness of vacuum sintered